Solid State Communications ■ (■■■■) ■■■–■■■

Contents lists available at ScienceDirect

Solid State Communications

journal homepage: www.elsevier.com/locate/ssc

Thermal annealing and air exposing effect on the graphene/silicon Schottky junctions

Xiaojuan Wang [a,b], Yuanyuan Wang [c,*], Dong Li [a], Liping Zou [a], Qichong Zhang [a], Jun Zhou [a], Dongfang Liu [d,*], Zengxing Zhang [a,*]

[a] MOE Key Laboratory of Advanced Micro-structured Materials & Shanghai Key Laboratory of Special Artificial Microstructure Materials and Technology, School of Physics Science and Engineering, Tongji University, Shanghai 200092, China
[b] School of Physics and Electronics, Henan University, Kaifeng 475004, China
[c] School of Urban Development and Environment Engineering, Shanghai Second Polytechnic University, Shanghai 201209, China
[d] Shanghai Advanced Research Institute, Chinese Academy of Sciences, Shanghai 201210, China

ARTICLE INFO

Article history:
Received 7 September 2014
Received in revised form
22 October 2014
Accepted 24 October 2014
Communicated by F. Peeters

Keywords:
A. Grapheme
A. Shottky junction
D. Electronic
D. Optoelectronic

ABSTRACT

Graphene/silicon (Gr/Si) configurations form Schottky junctions and should be a promising structure for high-performance electronics and optoelectronics. Here we presented a study on the properties of Gr/Si Schottky junctions by thermal annealing and air exposing. It was found that the ideal factor and the Schottky barrier height were lowered after vacuum annealing and increased after exposing in air for several days. The modulation of the Schottky junctions was further used to tune their optoelectronic properties. The results exhibit that the open-circuit voltage of the junctions under light illumination was varied with the ideal factor. The work here should be helpful on developing high-performance Gr/Si electronics and optoelectronics.

1. Introduction

Graphene has a unique two-dimensional (2-D) structure and excellent properties of high optical transparency, in-plane good conductivity, and exceptional mechanical stability, making it a promising candidate for the future flexible transparent electrodes [1–4]. It is thus stimulating great interest to develop suitable method to get high-performance graphene transparent electrodes and apply them for variable devices, including solar cells, light-emitting diodes (LEDs), photodetectors, touch screens, and so on [5–9]. On the other hand, silicon is a versatile semiconductor and widely used for optoelectronics in industry. Therefore, the combination of graphene and silicon for optoelectronics is attracting especial attention. While graphene is covered on silicon, they form Schottky junctions and can be used for photovoltaic devices. Recently, Li et al. reported that graphene/silicon (Gr/Si) Schottky junctions could be employed as solar cells with the solar energy conversion efficiency of up to 1.7% [10]. Miao et al. achieved Gr/Si Schottky junction solar cells that exhibit a power conversion efficiency of 8.6% by doping graphene with bis-(trifluoromethanesulfonyl) amide [11]. Shi et al. involved a colloidal antireflection coating onto Gr/Si structures and enhanced the cell efficiency to 14.5% [12]. Besides solar cells, Gr/Si configuration used for photoelectrical detection also made great progress. An et al. reported Gr/Si junctions to be excellent weak-light detectors with a photovoltage responsivity exceeding 10^7 V/W, indicating that they should be a potential use for ultrasensitive photodetectors [13]. These excited results make the scientific community further study the properties of the Gr/Si Schottky junctions to finely modulate their electronic and optoelectronic properties.

Chen et al. studied the temperature dependent electronic properties of Gr/Si junctions, and simply involved the vacuum annealing effect on the devices [14]. In order to deeply understand the electronic properties and exploit their applications, further studies are important. In this study, the Gr/Si junctions were fabricated with *n*-type silicon and chemical vapor deposition derived monolayer graphene. Thermal annealing effect on the electronic properties, such as ideality factor, barrier height, series resistance, was studied in details. We also studied air exposing effect on these properties, which is important for real applications. One of the important applications for Gr/Si junction is optoelectronics. We further studied thermal annealing and air exposing effect on the photoelectrical properties of the Gr/Si junctions.

* Corresponding authors. Tel./fax: +86 2165983108.
E-mail addresses: wangyuanyuan@sspu.edu.cn (Y. Wang), liudf@sari.ac.cn (D. Liu), zhangzx@tongji.edu.cn (Z. Zhang).

http://dx.doi.org/10.1016/j.ssc.2014.10.028
0038-1098/

2. Experimental section

Graphene was synthesized with a chemical vapor deposition (CVD) method on Cu foils as what was reported [15]. After the furnace was heated up to 1000 °C and evacuated to less than 100 mTorr, Cu foils were loaded into the temperature zone. In the following, 100 SCCM H_2 was introduced in for 30 min, and then 10 SCCM CH_4 was added for another 30 min. After CH_4 was shut down, the Cu foils were taken out and cooled down to room temperature. Graphene was then obtained on the Cu foils. In order to transfer graphene, poly-methyl methacrylate (PMMA) was spin-coated on the as-produced Cu foils and baked at 120 °C for 1 min. The Cu foils were then removed by etching in an aqueous solution of 0.1 M $(NH_4)_2S_2O_8$ overnight [16]. After the Cu foils were dissolved thoroughly, graphene/PMMA films were rinsed three times with deionized (DI) water and then transferred on the specified substrates for characterization.

The Gr/Si configurations were fabricated as what was reported in the previous work [13]. The (001) silicon used here was of *n*-type with a resistivity of 1–10 Ω•cm and covered with a 300-nm-thick thermal oxide film. The thermal oxide film on the backside was firstly etched and covered with thermally deposited Au/Ni film, which was annealed previously to form Ohmic contact to the Si [17]. Standard photolithography and wet etching (by buffered oxide etchant, BOE) method was employed to etch the SiO_2 on the topside with a square area of 0.1 cm^2 in the center of the wafers. After the underneath silicon present, it was rinsed with deionized (DI) water, dried by nitrogen gas flow, and rapidly covered with graphene film contacting with previously deposited Au/Ni electrodes around the etched window. It should be noted here that the PMMA on the graphene is carefully removed by acetone after the whole process. Schematic plans and photograph of the produced Gr/Si heterostructures is shown in Fig. 1(a).

The Raman spectra were measured by a Horiba Jobin Yvon LabRAM HR800 Raman system with a 514-nm laser. The electrical and photoelectrical properties were characterized with a Keithley 4200-SCS semiconductor analyzer. The light source was a light-emitting diode (LED) lamp whose power can be modulated. We used an optical power meter of SGN-1 to measure the power of the light and calculated the incident power on the junctions according to their area.

3. Results and discussion

Fig. 1(a) shows schematic plans and a photograph of Gr/Si junctions. Fig. 1(b) shows typical Raman spectra of the transferred graphene in an as-produced Gr/Si configuration excited with a laser wavelength of 514 nm at room temperature. Raman spectroscopy is a powerful tool to characterize the properties of graphene. The intensity of the D band is dependent on both of defects and doping level in graphene [18]. Our results demonstrate that the D band of the produced graphene is nearly free, indicating that the graphene should have a high quality. The intensity of the 2D band is around twice of the G band, exhibiting that it should be monolayer graphene [15]. The Raman spectrum on the etched silicon window shows an intensity at around 1430 cm^{-1}, which can be ascribed to the underneath silicon [19]. Combining the photograph result in Fig. 1(a), we can get the conclusion that the monolayer graphene is covered on the etched silicon structure.

The electronic properties of the as-produced Gr/Si configurations are characterized by a Keithley 4200-SCS semiconductor analyzer at room temperature in atmosphere. Fig. 1(c) shows the current–voltage (*I*–*V*) curve of a typical Gr/Si junction under dark condition. The *I*–*V* curve exhibits an obvious rectifying behavior and demonstrates that the Gr/Si configurations are well-defined Schottky diodes with a rectification ratio of $10^4 \sim 10^6$. The electronic properties of the Schottky junctions are demonstrated by their intrinsic parameters, such as ideality factor (n), Schottky barrier height (Φ_B) and series resistance (R_S), which can be extracted from a single *I*–*V* curve. The forward current across a Schottky junction follows the thermionic emission model expressed with the equations of [20]

$$I = I_S\left[\exp\left(\frac{eV_D}{nkT} - 1\right)\right], \tag{1}$$

$$V_D = V - IR_S, \tag{2}$$

where e is the electronic charge, V_D is the bias voltage applied across the junction, n is the ideality factor characterizing the junction performance, k is the Boltzmann constant, and T is the absolute temperature. I_S is the reverse saturation current, which can be expressed with

$$I_S = A_{\text{eff}}A^{**}T^2\exp\left(-\frac{e\Phi_B}{kT}\right), \tag{3}$$

where A_{eff} is the effective junction area, A^{**} is the Richardson constant, and Φ_B is the Schottky barrier height. Defining the current density J as I/A_{eff}, the following equations can be deduced from eqs. (1), (2) and (3),

$$\frac{d(V)}{d(\ln J)} = R_S A_{\text{eff}} J + \frac{kT}{e}n. \tag{4}$$

$$H(J) = R_s A_{\text{eff}} J + n\Phi_B. \tag{5}$$

Here $H(J)$ is defined as

$$H(J) = V - \frac{nkT}{e}\ln\frac{J}{A^{**}T^2}. \tag{6}$$

From the linear equations of (4) and (5), n, Φ_B and R_S can be obtained easily. Fig. 1(d) is the corresponding d*V*/dln(*J*)–*J* and H(*J*)–*J* curves. Combining the Eqs. (4) and (5), n, Φ_B and R_S can be obtained as 1.75, 0.81 eV and 660 Ω, respectively.

Vacuum annealing could improve the performance of electronic devices. We thus studied the property variation of the Gr/Si devices under vacuum annealing at 300 °C in the protection with H_2 for 1 h. Fig. 2(a) shows typical *I*–*V* characteristic curves of a same junction before and after vacuum annealing and again-exposed in air for 5 days at room temperature. Compared with the as-produced junction, the as-annealed junction shows a lower turn-on voltage and a bigger forward current. However, after a long time exposure in air for 5 days, the turn-on voltage is surprisingly recovered even with a little bigger. In order to better understand the variation of the *I*–*V* curves, we studied the intrinsic parameters of the Schottky junctions carefully. Fig. 2(b) shows the variation of n, Φ_B and R_S with different processing conditions. These parameters are obtained with the same method as demonstrated above. Obviously, vacuum annealing could lower all of the three parameters of n, Φ_B and R_S. But after being exposed in air for several days, they increase slowly. The turn-on voltage of the Schottky junctions is dependent on the Φ_B. The higher Φ_B means that the charges could overcome a higher barrier resulting in the turn-on voltage bigger, and vice versa. Based on Eq. (1), the forward current is dependent on the n, Φ_B and R_S. The reduction of the three parameters would lead to a high forward current. This could be used to explain the variation of the *I*–*V* curves under different processing conditions. The results demonstrated above mean that vacuum annealing has an obvious effect on the properties of the Gr/Si Schottky junctions. The lower ideality factor means that the Gr/Si has a better Schottky contact. The results indicate that vacuum annealing could improve the Schottky junction, but air-exposing decreases the properties.

Please cite this article as: X. Wang, et al., Solid State Commun (2014), http://dx.doi.org/10.1016/j.ssc.2014.10.028

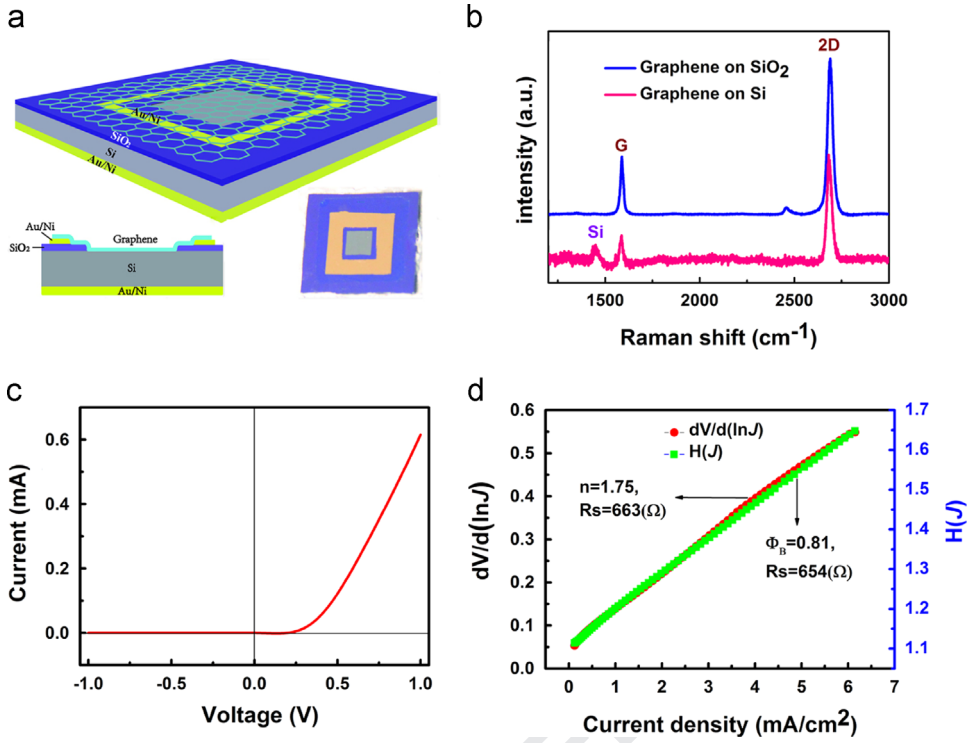

Fig. 1. (Color online) (a) Photograph and schematic plans of the produced Gr/Si configurations. (b) Raman spectra of the graphene on SiO_2 and Si, respectively. (c) Typical *I*–*V* curve of an as-produced Gr/Si junction under dark condition. (d) d*V*/d(ln*J*)–*J* and *H*(*J*)–*J* curves, from which ideal factor (*n*), Schottky barrier height (Φ_B) and series resistance (R_S) can be extracted.

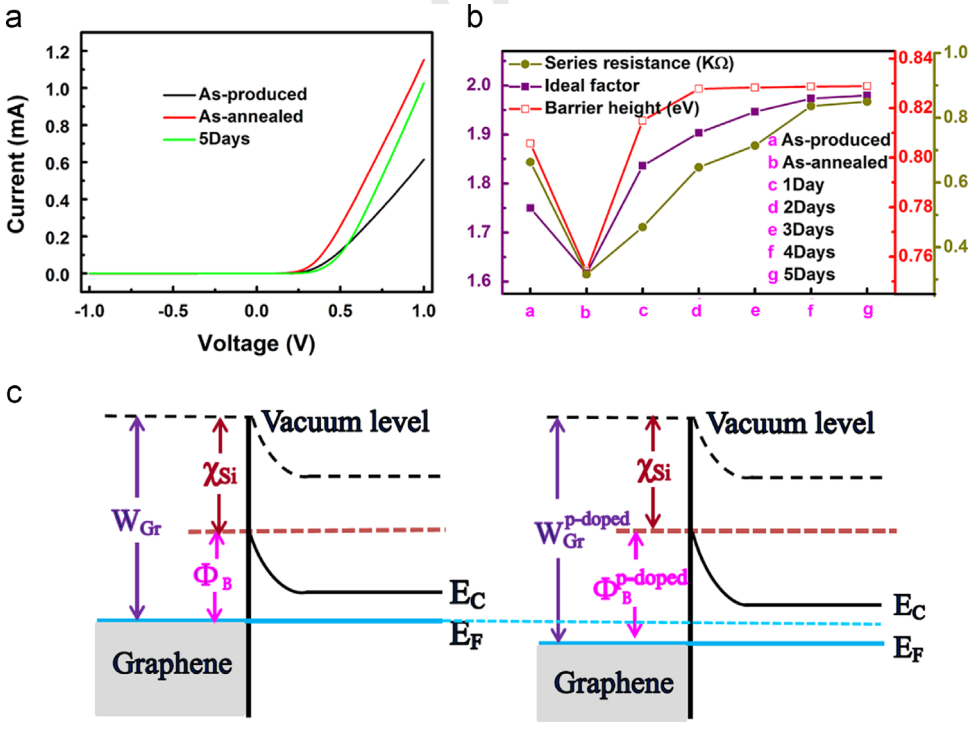

Fig. 2. (Color online) (a) Dark *I*–*V* curves of a same Gr/Si Schottky junction with different processing conditions, (b) ideality factors (*n*), Schottky barrier height (Φ_B) and series resistance (R_S) of the Schottky junction varying with different processing conditions. Here 1 day means that the junction is exposed in air for 1 day after annealing, and so forth and (c) energy band diagram of an ideal Schottky junction. The left is for intrinsic graphene, and the right is for *p*-doped graphene.

Fig. 2(c) shows the energy band diagram of the Gr/*n*-Si Schottky junction. The barrier height (Φ_B) of the junction is dependent on the difference of the graphene working function (W_{Gr}) and the silicon electron affinity (χ_{Si}). While graphene is exposed in air, oxygen or water molecules are often absorbed on the surface of graphene making it *p*-doped [21–24]. This would make the graphene working function increasing and result in the Φ_B raising [9,11]. Vacuum annealing could make desorption of these molecules, and thus decreases Φ_B. While these junctions are exposed in air again, these molecules could be absorbed on the

Please cite this article as: X. Wang, et al., Solid State Commun (2014), http://dx.doi.org/10.1016/j.ssc.2014.10.028

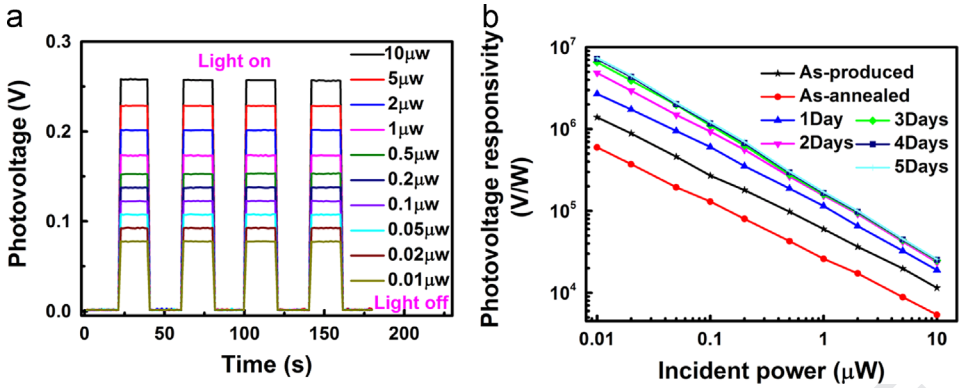

Fig. 3. (Color online) Photodetective properties of Gr/Si Schottky junctions. (a) Photovoltage response of the junction to the light with different powers switching on and off; the photovoltage is of open-circuit voltage, V_{OC} and (b) variation of the photovoltage responsivity as a function of incident power.

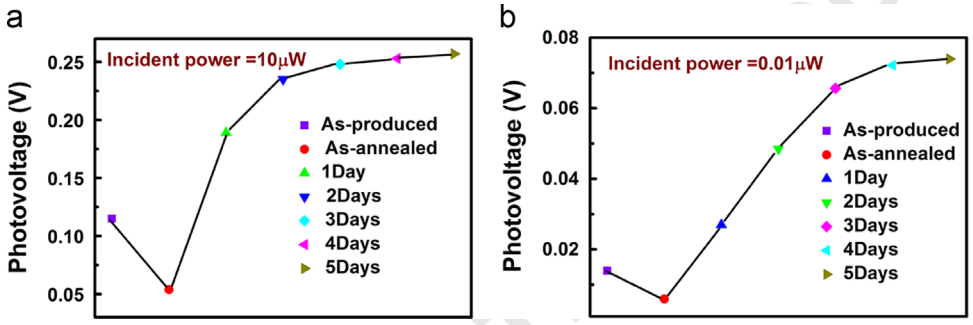

Fig. 4. (Color online) The open-circuit voltages (V_{OC}) of the Schottky junction with different processing conditions. The incident light power is (a) 10 μW, and (b) 0.01 μW. Here 1 day means that the junction is exposed in air for 1 day after annealing, and so forth.

graphene surface again. This should be the reason of the recovery of Φ_B. It should be noted here that it is well-known that silicon would be oxidized with a thin oxide layer covered if it is exposed in air. CVD-derived graphene often has defects [25–27]. This should lead to oxygen molecules diffusing onto the silicon resulting in a thin oxide layer formed on the surface [14,28]. It would make the Gr/Si junction form a graphene-oxide-silicon structure. The later structure often has a bigger Φ_B and a higher R_S, and increases n too.

Due to being sensitive to visible light, Gr/Si Schottky junctions can be employed for photodetectors [8,13]. We further studied the photodetective properties of the Gr/Si junctions. Fig. 3(a) shows time-resolved photovoltage response of a 5-days-air-aged junction to the light with different powers switching on and off for four cycles. It clearly exhibits that the photovoltage is produced while the light switches on, and rapidly disappears while the light switches off. The produced photocurrent increases with the light enhancing. Here, the photovoltage is the open-circuit voltage of V_{OC} with a bias current of 0. The light source is a white light-emitting diode (LED) lamp whose power can be modulated. We further studied the photovoltage responsivity of the junctions and the results are shown in Fig. 3(b). Under the incident light power of 0.01 μW, the photovoltage responsivity is almost 10^7 V/W. The high responsivity makes the junctions promising to detect weak light signals. Here the photovoltage responsivity is defined as V_{OC}/P. P is the incident light power.

For Schottky junctions, I–V characteristic under light illumination follows the equation of [29]

$$I = I_S\left[\exp\left(\frac{eV}{nkT}\right) - 1\right] - I_L, \tag{7}$$

where n is the ideality factor, I_S is the reverse saturation current and I_L is the current from the excess photo-excited carriers. V_{OC} is defined as that the bias current of I is 0. From eq. (7), V_{OC} can be deduced as

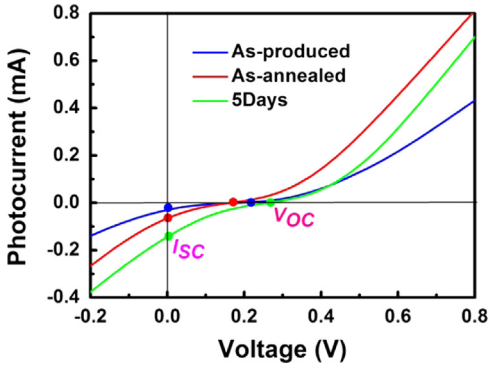

Fig. 5. (Color online) Light I–V curves of a same Gr/Si Schottky junction with different processing conditions. Here the incident power is 10 μW.

$$V_{OC} = \frac{nkT}{e}\ln\left(1 + \frac{I_L}{I_S}\right). \tag{8}$$

Therefore, for a given I_L, V_{OC} is mainly dependent on the ideality factor n, indicating that the V_{OC} can be modulated by varying the ideality factor. Fig. 4 shows the variation of the V_{OC} with different processing conditions. It demonstrates that the open-circuit voltage (V_{OC}) decreases after vacuum annealing and increases again after again-exposed in air for several days. The variation behavior is almost similar to the ideality factor, indicating that the V_{OC} can be modulated by the ideality factor. The modulation effect on the V_{OC} is also exhibited on the photovoltage responsivity. In Fig. 3(b), it clearly indicates that the photovoltage responsivity is varied with different processing conditions that are according to different ideality factors. It should be noted here that the modulation effect on the V_{OC} by the ideality factor seems to be dependent on the

light power. Under the low light power, the variation of the V_{OC} is more obvious, as shown in Fig. 4(a) and (b).

Fig. 5 shows the *I–V* curves of a same Gr/Si Schottky junction under light illumination with different processing conditions. The results clearly exhibit that the V_{OC} decreases after vacuum annealing, but increases after being exposed in air for 5 days. However, the short-circuit current (I_{SC}) keeps on increasing in the sequence of as-produced, as-annealed and being exposed in air for 5 days. Under the light illumination of 10 μW, the fill factor of them is around 0.15, 0.18, and 0.16 in sequence. It is inversely dependent on the ideality factor, which should be due to the variation of the recombination pathways at the interface. However, the results indicate that the conversion efficiency is enhanced successively.

4. Conclusion

In summary, by using CVD-derived graphene and *n*-type silicon, we fabricated graphene/silicon (Gr/Si) configurations for Schottky junctions. The electronic properties of the junctions can be modulated by vacuum annealing or exposing in air. The results exhibit that vacuum annealing decreases the series resistance (R_S), the ideal factor (n) and the Schottky barrier height (Φ_B). After exposing in air for several days, R_S, n and Φ_B are enhanced again. The variation of these parameters is ascribed to the desorption or adsorption of the water or oxygen molecules in air, and possible oxidization of the interface silicon. The Gr/Si junctions are further developed for optoelectronics. The results exhibit that the open-circuit voltage of the Schottky junctions is varied with the ideality factor. The presented work here should be helpful on developing high-performance Gr/Si electronics or optoelectronics.

Acknowledgments

The work was supported by NSFC (11104204), Shanghai Pujiang Program (12PJ1408900). School Foundation of Shanghai Second Polytechnic University (EGD13XQD15), and Shanghai Excellent Young Teacher Foundation (ZZEGD13019).

References

[1] A.K. Geim, K.S. Novoselov, Nat. Mater. 6 (2007) 183–191.
[2] K.S. Novoselov, V.I. Fal'ko, L. Colombo, P.R. Gellert, M.G. Schwab, K. Kim, Nature 490 (2012) 192–200.
[3] R. Nair, P. Blake, A. Grigorenko, K. Novoselov, T. Booth, T. Stauber, N. Peres, A. Geim, Science 320 (2008) (1308-1308).
[4] K.I. Bolotin, K.J. Sikes, Z. Jiang, M. Klima, G. Fudenberg, J. Hone, P. Kim H.L. Stormer, Solid State Commun. 146 (2008) 351–355.
[5] C.-L. Hsu, C.-T. Lin, J.-H. Huang, C.-W. Chu, K.-H. Wei, L.-J. Li, ACS Nano 6 (2012) 5031–5039.
[6] V.C. Tung, L.-M. Chen, M.J. Allen, J.K. Wassei, K. Nelson, R.B. Kaner, Y. Yang, Nano Lett. 9 (2009) 1949–1955.
[7] Z. Liu, Q. Liu, Y. Huang, Y. Ma, S. Yin, X. Zhang, W. Sun, Y. Chen, Adv. Mater. 20 (2008) 3924–3930.
[8] Z. Zhang, Y. Guo, X. Wang, D. Li, F. Wang, S. Xie, Adv. Funct. Mater. 24 (2014) 835–840.
[9] S. Bae, H. Kim, Y. Lee, X. Xu, J.-S. Park, Y. Zheng, J. Balakrishnan, T. Lei, H.R. Kim, Y.I. Song, Nat. Nanotechnol 5 (2010) 574–578.
[10] X. Li, H. Zhu, K. Wang, A. Cao, J. Wei, C. Li, Y. Jia, Z. Li, X. Li, D. Wu, Adv. Mater. 22 (2010) 2743–2748.
[11] X. Miao, S. Tongay, M.K. Petterson, K. Berke, A.G. Rinzler, B.R. Appleton A.F. Hebard, Nano Lett. 12 (2012) 2745–2750.
[12] E. Shi, H. Li, L. Yang, L. Zhang, Z. Li, P. Li, Y. Shang, S. Wu, X. Li, J. Wei, K. Wang, H. Zhu, D. Wu, Y. Fang, A. Cao, Nano Lett. 13 (2013) 1776–1781.
[13] X. An, F. Liu, Y.J. Jung, S. Kar, Nano Lett. 13 (2013) 909–916.
[14] C.-C. Chen, M. Aykol, C.-C. Chang, A. Levi, S.B. Cronin, Nano Lett. 11 (2011) 1863–1867.
[15] X. Li, W. Cai, J. An, S. Kim, J. Nah, D. Yang, R. Piner, A. Velamakanni, I. Jung, E. Tutuc, S.K. Banerjee, L. Colombo, R.S. Ruoff, Science 324 (2009) 1312–1314.
[16] Z. Yan, J. Lin, Z. Peng, Z. Sun, Y. Zhu, L. Li, C. Xiang, E.L. Samuel, C. Kittrell J.M. Tour, ACS Nano 6 (2012) 9110–9117.
[17] T. Morimoto, T. Ohguro, S. Momose, T. Iinuma, I. Kunishima, K. Suguro, I. Katakabe, H. Nakajima, M. Tsuchiaki, M. Ono, IEEE Trans.Electr. Dev. 42 (1995) 915–922.
[18] J. Liu, Q. Li, Y. Zou, Q. Qian, Y. Jin, G. Li, K. Jiang, S. Fan, Nano Lett. 13 (2013) 6170–6175.
[19] O. Ochedowski, G. Begall, N. Scheuschner, M. El Kharrazi, J. Maultzsch, M. Schleberger, Nanotechnology 23 (2012) 405708.
[20] S.K. Cheung, N.W. Cheung, Appl. Phys. Lett. 49 (1986) 85–87.
[21] A. Pirkle, J. Chan, A. Venugopal, D. Hinojos, C. Magnuson, S. McDonnell, L. Colombo, E. Vogel, R. Ruoff, R. Wallace, Appl. Phys. Lett. 99 (2011) 122108.
[22] Z.H. Ni, H.M. Wang, Z.Q. Luo, Y.Y. Wang, T. Yu, Y.H. Wu, Z.X. Shen, J. Raman Spectrosc. 41 (2010) 479–483.
[23] H. Liu, Y. Liu, D. Zhu, J. Mater. Chem. 21 (2011) 3335–3345.
[24] K.S. Novoselov, A.K. Geim, S. Morozov, D. Jiang, Y. Zhang, S. Dubonos, I. Grigorieva, A. Firsov, Science 306 (2004) 666–669.
[25] J.W. Suk, A. Kitt, C.W. Magnuson, Y. Hao, S. Ahmed, J. An, A.K. Swan B.B. Goldberg, R.S. Ruoff, ACS Nano 5 (2011) 6916–6924.
[26] Q. Yu, L.A. Jauregui, W. Wu, R. Colby, J. Tian, Z. Su, H. Cao, Z. Liu, D. Pandey, D. Wei, Nat. Mater. 10 (2011) 443–449.
[27] Y. Zhang, T. Gao, Y. Gao, S. Xie, Q. Ji, K. Yan, H. Peng, Z. Liu, ACS Nano 5 (2011) 4014–4022.
[28] Y.-J. Lin, J.-H. Lin, Appl. Surf. Sci. 311 (2014) 224–229.
[29] S.M. Sze, K.K. Ng, John Willey & Sons, Inc.: Hoboken, New Jersey, 2007, pp 733–734.

Please cite this article as: X. Wang, et al., Solid State Commun (2014), http://dx.doi.org/10.1016/j.ssc.2014.10.028